EFFECT OF DIFFERENT WEIGHT PERCENTAGES OF WASTE TIRE RECOVERED CARBON BLACK (RCB) ON THE STRUCTURAL AND MORPHOLOGICAL PROPERTIES OF GRAPHENE OXIDE (GO)

Azra Umairah Anuar[1], Noor Najmi Bonnia[1,2,*], Norashirene Mohamad Jamil[1], Nor Suhaila Mohamad Hanapi[1], Engku Zaharah Engku Zawawi[1] and Nor Dalila Nor Affandi[1,2]

[1]Faculty of Applied Sciences, Universiti Teknologi MARA, 40450 Shah Alam, Selangor, Malaysia.
[2]Textile Research Group, Faculty of Applied Sciences, Universiti Teknologi MARA, 40450 Shah Alam, Selangor, Malaysia.

*noornajmi@uitm.edu.my

Abstract. Graphene oxide (GO) is a promising material useful in energy storage applications, sensors, supercapacitors, solar cells, and biomedical applications. However, the mining process of graphite as raw material for GO is complicated and can harm the environment and local communities. Besides, GO is currently regarded as an expensive material due to its complicated manufacturing method and limited production capacity. For this purpose, recovered carbon black (rCB) of waste was used to synthesize GO by utilizing the modified Hummers method and characterized by Raman spectroscopy, X-ray diffraction (XRD), Fourier transform infrared spectroscopy (FT-IR), and field emission scanning electron microscope (FESEM). Raman analysis showed D-band peaks at 1359 cm^{-1}, 1357 cm^{-1}, and 1355 cm^{-1} and G-band peak at 1618 cm^{-1}, 1585 cm^{-1}, and 1583 cm^{-1} for GO-1%, GO-3%, and GO-5% respectively indicate the successful synthesis of GO. The intensity ratio (I_d/I_g) of GO-3% was the highest with I_d/I_g of 0.82 indicating the highest oxidation degree. The FT-IR spectroscopy showed the presence of OH, C=O, and C-O stretching vibrations on the structure of GO-1%, GO-3%, and GO-5%, suggesting successful of oxidation process in converting rCB to GO. XRD analysis shows the peak appear at 2θ = 25.33°, 25.54°, and 25.56° for GO-1%, GO-3%, and GO-5% respectively. Moreover, FESEM analysis shows that the smallest mean particle size was obtained for GO-3% at the range of 20~40 nm.

Keywords: Graphene oxide, waste tire, carbon, Hummers' method

Article Info

Received 2nd January 2024
Accepted 14th May 2024
Published 12th June 2024

ISSN: 1823-7010, eISSN: 2600-7444

1. INTRODUCTION

In recent decades, there has been a tremendous increase in interest in nanotechnology as a revolutionary field for advancing a wide range of scientific concerns. However, out of all the manufactured nanomaterials that are currently accessible, carbon-based nanostructures have drawn much attention, mainly because of the unique qualities of carbon and the efficacious effects that have been demonstrated. Graphene is one of the carbon nanomaterials that has become a two-dimensional substance comprised of sp^2 hybridized carbon tightly packed into a honeycomb pattern. Graphene was theorized to be the fundamental component of graphite in 1940, and Noveselov and Geim described a way to make a single graphene sheet in 2004 [1]. On the other hand, graphene oxide (GO) is a graphene-based material that demonstrates intriguing chemical, optical, and electrical properties due to the graphene skeleton and oxygen-containing functional groups found in the basal plane and at the edge of graphene sheets [2]. The features of GO, including its hydrophilicity and ease of modification to create other graphene-based materials, have generated significant attention. GO and GO-based nanomaterials exhibit crucial properties, making them a potential material for nanotechnology, including fuel cells, in vivo sensors, supercapacitors, energy storage, and electronics.

Recently, waste tires are a contemporary risk that poses a significant global challenge. Waste tires are still disposed of incorrectly despite recycling efforts and laws at state and federal levels of government [3]. To reduce the negative environmental impacts of waste tires, it is crucial to comprehend the significance of recycling discarded tires after they are removed from cars and reduce the accumulation of waste at the dump sites. Pyrolysis is a sustainable process that can convert and repurpose the waste tires into recovered carbon black (rCB). The rCB extracted from waste tires serves as a potential carbon source in the production of GO. This process not only alleviates the environmental burden of tire disposal but also transforms a readily available waste into a valuable resource, thus promoting resource efficiency and reducing the need for graphite as a raw material to synthesize GO.

The existing body of research on the factors influencing the structural and morphological properties of GO has revealed valuable insights. For example, enhancing the intercalator and oxidant dosages can elevate the oxidation degree of GO, aiding in the production of conventional GO with increased interlayer spacing [4]. However, they should have delved into the nuanced variations that arise with different weight percentages of the raw material. Similarly, extending the reaction time led to a substantial increase in exfoliation, while the chemical composition of the resulting GO remained consistent, indicating that longer reaction times yield large and well-exfoliated GO flakes without sacrificing their chemical integrity [5]. Nonetheless, a noticeable research gap remains in our understanding of the intricate relationship between varying weight percentages of raw material, explicitly using recovered carbon black, to the structural and morphological properties of the synthesized GO by using the modified Hummers' method.

To the best of our knowledge, there is currently limited literature available that explores the impact of varying weight percentages of raw materials on the structural and morphological characteristics of GO. This research seeks to bridge the gap by offering a comprehensive investigation into the influence of different weight percentages of rCB from waste tires as alternative source materials on the structural and morphological properties of GO. By assessing these properties across a range of weight percentages, this study aims to

contribute a valuable insight essential for tailoring GO to meet the specific requirements for diverse research applications.

2. MATERIALS AND METHODS

2.1 Synthesis of GO using Modified Hummers' Method

The GO was synthesized based on the previous method described by our previous work [6]. GO was synthesized by the oxidation process of rCB from waste tire through a modified Hummers method. In brief, 1 wt% of rCB from the waste tire was introduced to 23 mL sulphuric acid (H_2SO_4) 1.0 g of sodium nitrate ($NaNO_3$). Then, 3.0 g of potassium permanganate ($KMnO_4$) was slowly added to the mixture and stirred for 1 hour under 20 ºC. The ice bath was removed, and the mixture was allowed to cool at room temperature for 16 hours. The mixture was then heated to 35 ºC and stirred for another hour. 46 mL of distilled water was added to the mixture while it was being heated to 90 ºC and stirred for two hours. The heater was turned off, after which the liquid-cooled to room temperature. Next, 100 mL of distilled water was added to the mixture and was agitated for 1 hour. To remove the extra $KMnO_4$, 10 mL of 30% H_2O_2 was added gradually and agitated for 1 hour. Then, the solution of 1:3 of HCl to distilled water was used to separate the precipitate from the liquid. The obtained precipitate was heated using an oven at 70 ºC for 24 h to produce GO powder. By replacing 1 wt% of rCB with 3 and 5 wt% of weight percentages, GO from different weight percentages of rCB was created using the same technique. For GO created from rCB with weight percentages of 1%, 3%, and 5%, respectively, the produced sample was designated GO-1%, GO-3%, and GO-5%.

2.2 Material Characterizations

Raman spectroscopy (Horiba Jobin-Yvon LabRam HR800) with laser excitation wavelength of 532 nm and integration duration of 5.03645 seconds was used to determine the structural analysis of the rCB and GO samples. The X-ray diffraction (XRD) patterns were obtained by using Cu Kα radiation (λ=1.5406 Å) with an acceleration voltage of 40 kV and a current of 20 mA, on a Rigaku Rigaku-Denki (Geigerflex). Using the Perkin Elmer Spectrum 400 ATR-FTIR, the FTIR spectra of the rCB and the GO samples were obtained at a resolution of 16 cm-1 for a frequency of 20 kHz, ranging from 500 to 4000 cm-1. Field emission scanning electron microscope (Model: JSM - 7600F, Brand: Jeol) was used to analyse the surface morphology of the rCB and GO samples. The samples were placed on a holder after being thinly coated with gold-palladium (Au-Pd) to ensure a clear and accurate image.

3. RESULTS AND DISCUSSION

3.1 Raman Spectroscopy Analysis

Raman spectroscopy is an efficient, non-destructive technique commonly used to determine the structural defect and degree of graphitization of carbon-based materials, such as GO and carbon compounds. In this study, the intensity of the I_d/I_g ratio was utilized to determine the quality of carbon materials through the degree of oxidation process. G-band peak rise was attributed to the in-plane vibrations induced by sp^2-bonded carbon atoms. In contrast, the D-band peak rise was attributed to out-plane vibrations caused by the structural

flaw in carbon materials. Meanwhile, the 2D- band can provide the number of graphene layers of the GO [7].

Figure 1 displays the dominant D-band, G-band and 2D-band emitted by GO with three different percentages of rCB. Based on the table 1, the D-band was observed at peaks 1359, 1357, and 1355 cm^{-1} for GO-1%, GO-3%, and GO-5%, respectively. The G-band for GO-1%, GO-3%, and GO-5% samples were recorded at 1618, 1585, and 1583 cm^{-1}, respectively.

Table 1: The Raman spectra of GO obtained at different weight percentages compared with the reference result of GO produced from commercial graphite [8]

Sample	D-band (cm^{-1})	G-band (cm^{-1})
Reference	1324	1599
GO-1%	1359	1618
GO-3%	1357	1585
GO-5%	1355	1583

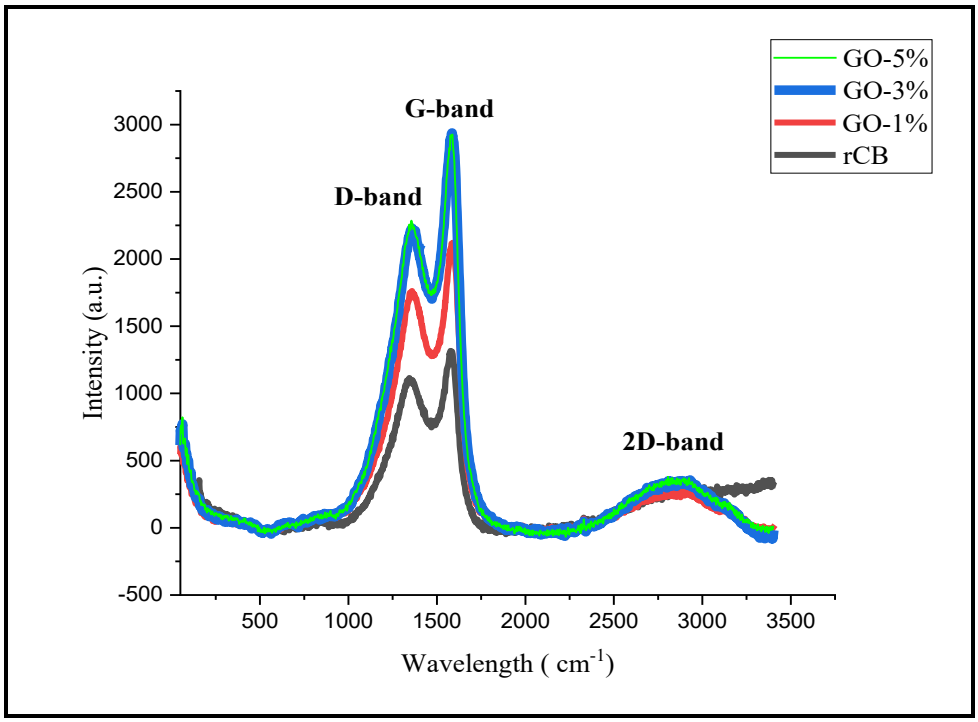

Figure 1: Raman spectra result obtained for GO-1%, GO-3%, and GO-5%

The observed G-band and D-band peaks for all three samples with various weight percentages similar to the peak of GO from pristine graphite thus confirmed that the samples produced were GO [9]. Figure 1 shows that the D-band peak for each sample was obtained at different intensities. The increase in the intensity of the D-band was due to the structural defect disorder of the graphitic domain generated by the addition of oxygenated functional groups (such as hydroxyl, carboxyl, and epoxy groups) during the oxidation process. While G-band intensity is due to the first-order scattering of E_{2g} phonons from sp^2 carbon atoms. The G-band peaks of GO-1%, GO-3%, and GO-5% were observed at 1602, 1593 and 1589 cm^{-1} respectively. Next, the 2D- peak in the Raman spectrum of GO can provide information

about the layer number of the material. Figure 1 shows the broad and wide 2D peak for GO-1%, GO-3%, and GO-5%, indicating the produced samples are in multilayer. The interaction between layers of GO resulted in increased structural disorder and phonon scattering, leading to a broadening of the Raman peaks. Therefore, the broader and wider of 2D peak observed on the Raman spectra of GO-1%, GO-3%, and GO-5% indicates the presence of multiple layers within the GO samples, aligning with the characteristics expected for multilayer GO [10].

The intensity ratio (I_d/I_g) in Raman spectra of GO is a parameter commonly used to characterize the structural disorder and defects in graphene-based materials [11]. Table 2 demonstrates the calculated intensity ratio (I_d/I_g), and the number of layers for GO-based rCB of waste tires is 0.77, 0.82, and 0.73 for GO-1%, GO-3%, and GO-5%, respectively. The highest intensity ratio of I_d/I_g was observed for GO-3% compared to the other two samples. These indicate that the GO-3% undergoes the highest degree of oxidation and more introduction of defects in the structure of GO-3%. Table 1 shows that GO-3% has the highest concentration of oxygen-containing functional groups compared with the other two samples (GO-1% and GO-5%).

Table 2: The intensity ratio and the number of layers of the produced sample were compared with the reference result of GO produced from commercial graphite [12]

Sample	Intensity ratio (I_d / I_g)	Number of layers
Reference	0.86	Multilayer
GO-1%	0.77	Multilayer
GO-3%	0.82	Multilayer
GO-5%	0.73	Multilayer

3.2 X-ray Diffraction (XRD) Analysis

XRD was used to examine the crystalline structure, d-spacing (λ), and crystallite size (D) of rCB and GO. It can also determine the degree of crystallinity and identify the impurities in rCB and the produced samples. GO typically exhibits intense and prominent characteristic peaks at 2θ =10°, corresponding to the (001) lattice plane [13]. The d-spacing of the particle was calculated by Bragg's equation, as shown by equations 1 and 2.

$$2d \sin(\theta) = n\lambda \quad (1)$$

Then rearrange to be as follows:

$$d = \sin(\theta) / n\lambda \quad (2)$$

Figure 2 shows XRD patterns demonstrating the significant molecular change between the rCB waste tire pattern and the product synthesis. The major peak in rCB waste tire is at 2θ = 44.67° with some small peaks at 2θ of 28.67°, 38.43°, 47.76°, 56.67°, 65.04°, and 78.16°. Typically, XRD patterns of carbon black show a broad, diffuse scattering pattern due to the amorphous material nature of the material [14]. However, in the case of rCB, the XRD pattern shows some peaks that correspond to the crystalline impurities because of a sharp peak occurring on the microstructure of rCB as it was produced from waste materials. Meanwhile, a broad peak at 2θ= 25.88° indicates the presence of amorphous carbon, with the d-spacing at around 1.46 Å.

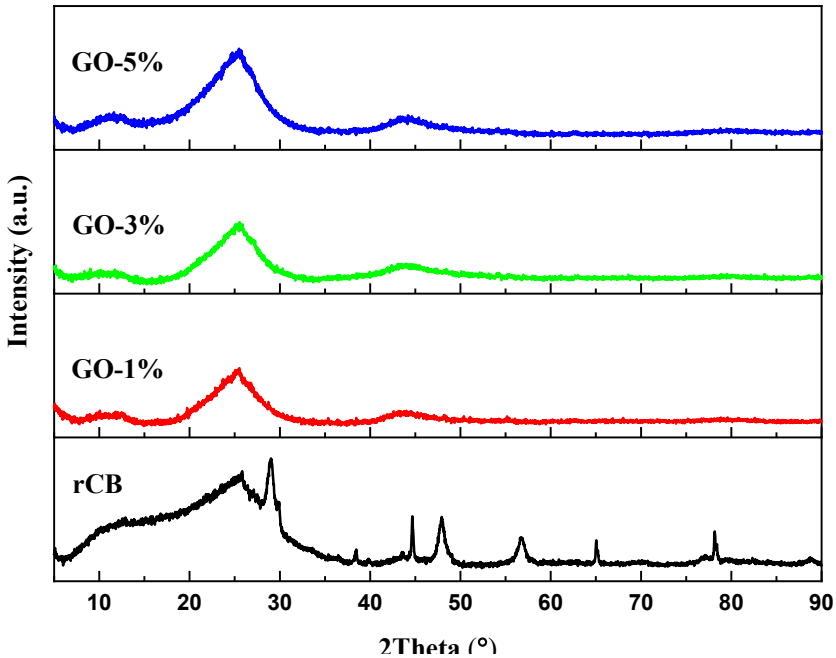

Figure 2: XRD spectra of rCB and graphene oxide (GO-1%, GO-3%, GO-5%)

Then, following the oxidation process, the distinctive peak of rCB at 2θ = 25.88° shifts to a lower angle with recorded values of 2θ = 25.53°, 2θ = 25.54°, and 2θ = 25.56° for GO-1%, GO-3%, and GO-5%, respectively. The shift in the XRD peak of rCB to a lower angle indicated an increase in the interlayer spacing or d-spacing between the GO sheets. This shift was attributed to the introduction of oxygen-containing functional groups during the synthesis process, leading to enhanced interlayer interactions. Furthermore, the increase in the interlayer spacing (d-spacing) between the GO layers was obtained for GO-1%, GO-3%, and GO-5 with values of 2.82, 2.93 and 1.86 Å, respectively. The increase in the interlayer distance in the GO sample due the penetration of the oxygen functional group and structural defects during the chemical oxidation process of rCB. The calculated d-spacing values align with the observed XRD peak shift, reinforcing the notion that the introduction of functional groups between the graphene layers result in a discernible expansion of the interlayer spacing in GO synthesized from rCB.

The broad and wide peak of rCB was attributed to the amorphous phase observed at 2θ= 25.82°. This situation is likely due to the amorphous nature of the material (rCB) itself. The rCB was a common filler material in rubber tires, comprises small, highly disordered carbon particles with very high surface area. The oxidation of rCB to GO can further increase disorder and introduce functional groups on the graphene lattice, leading to a highly disordered and mostly amorphous material. The XRD results demonstrated in this study are from previous studies [15], which have also demonstrated that the XRD peak of GO synthesis from carbonaceous waste material is 2θ= 23°- 26°.

3.3 Fourier-Transform Infrared Spectroscopy (FTIR) Analysis.

FTIR study was performed to assess the chemical change during the synthesis process of rCB to GO. The main oxygen-containing functional groups present on GO generated from graphite include hydroxyl (-OH), carboxyl (-COOH), and epoxy groups(C–O–C), resulting in

polar surface characteristics [16]. Figure 3 displays the FTIR spectra of all the GO obtained from three (3) different weight percentages of rCB from waste tires. For FTIR spectra of rCB, few functional groups were present on the layered carbon structure.

Next, with the oxidation process, the oxygen functional group was further increased in all GO-1%, GO-3%, and GO-5%. The graph displays broad peak wavelengths of 3392 (GO-1%), 3407 (GO-3%) and 3395 cm^{-1} (GO-5%) that fell between 3200 and 3550 cm^{-1} of the IR spectrum table on the surface of GO, correspond to the OH stretching and bending [17]. At the wavelength of 1740, 1746 and 1735 cm^{-1}, the prominent peak was observed on the FTIR spectra for the sample GO-1%, GO-3%, and GO-5% respectively. This peak revealed the presence of carboxyl group (C=O) associated with the carboxylic acid that exists at the edge of GO.

The absorption peak at 1210 (GO-1%), 1193 (GO-3%) and 1215 cm^{-1} (GO-5%), attributed to the epoxy groups, specifically C-O stretching [18]. The FTIR spectra of the GO samples were similar to previous reports in the literature [19]. The presence of polar groups (carboxyl and epoxy), and the presence of water (-OH functional groups), suggests the strong intercalation of oxygenated functional groups and successful oxidation process of rCB to GO. Table 3 summarize the presence of functional group obtained for different GO samples (GO-1%, GO-3%, and GO-5%)

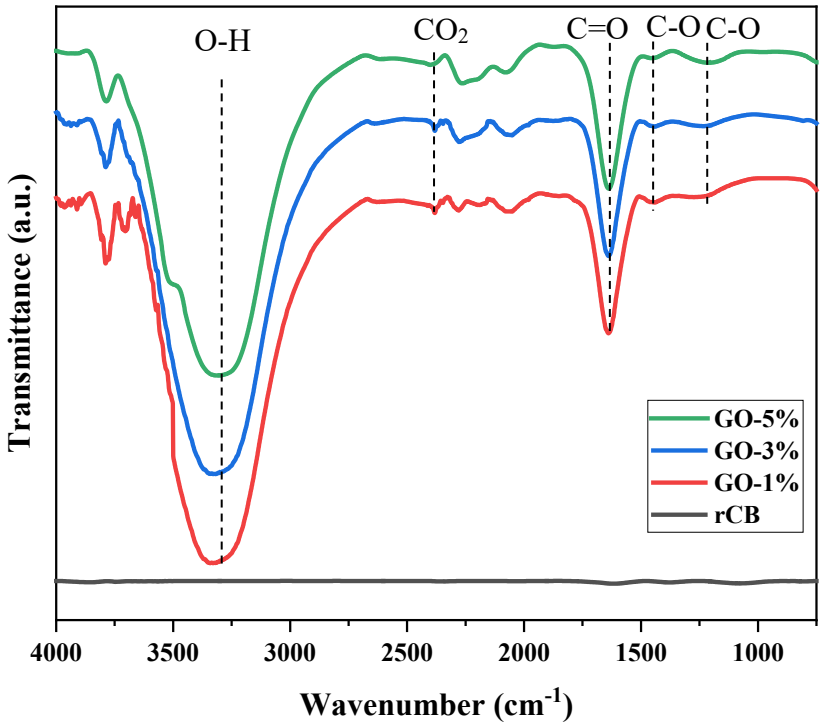

Figure 3: FTIR of rCB and GO samples (GO-1%, GO-3%, and GO-5%) after oxidation

Table 3: FTIR spectra obtained for the GO sample (GO-1%, GO-3%, and GO-5%) and the possible functional group

Reference (Wavenumber, cm^{-1})	GO-1% (Wavenumber, cm^{-1})	GO-3% (Wavenumber, cm^{-1})	GO-5% (Wavenumber, cm^{-1})	Functional group
3434.59	3392	3407	3395	O-H
2362.78	2381	2384	2394	CO_2
1726.10	1740	1746	1735	C=O
1387.41	1538	1430	1442	C-O
1110.80	1210	1193	1215	C-O

3.4 Morphological Analysis

The FESEM images in Figure 4 show the surface morphology of the GO samples. It can be seen that the grain's size of the GO-1%, GO-3%, and GO-5% nanoparticles is not uniform. Additionally, the grains of GO-1% appear clumped or glued together, which could be explained by the presence of oxygen-containing functional groups such as hydroxyl (-OH), carboxyl (-COOH), and epoxy (-O-) groups. These functional groups introduce polarity to the GO sheets, leading to increased intermolecular interactions such as hydrogen bonding and van der Waals forces, which can cause the sheets to aggregate or clump together. The graphene sheet is firmly linked, as evidenced by the morphology of GO-3%, which reveals that the grains are bound and aggregate. The GO surface topography and the quantity of GO layers in the sample are the following factors that contribute to the colour variation in FESEM. Next, the GO-5% grains appear to be densely packed, with less defect density appearing on the structure of GO-5%, indicating that less oxidation reaction occurs on the sample. This defect density could be referred to the irregular edges on the graphene sheets due to the oxidation process, which lead to the structural distortions on GO structure.

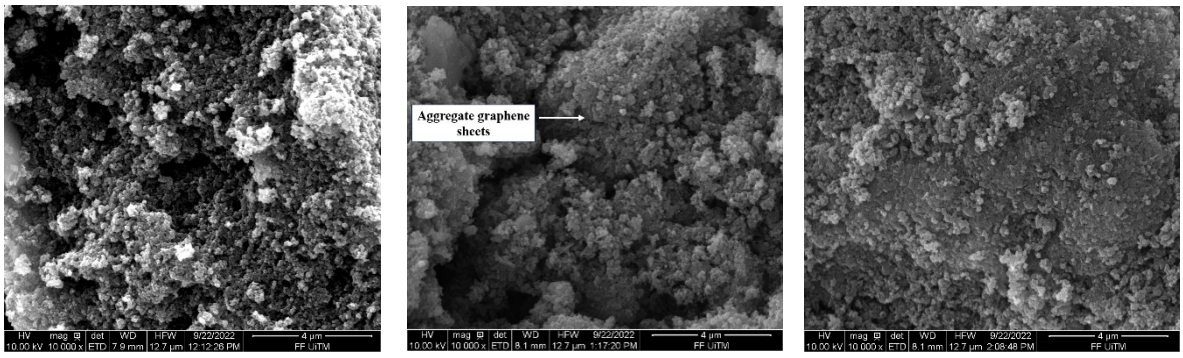

(a) *(b)* *(c)*

Figure 4: The FESEM images obtained at 10k x magnification for (a) GO-1%, (b) GO-3% and (c) GO-5%

In order to harness the optimal properties of GO, it is crucial for the particle size to be below 100 nm, as this categorizes it as a nanoparticle. At this scale, GO exhibits enhanced characteristics attributed to its nanomaterial nature, enabling superior performance in various applications. To determine the grain size of the samples, the frequency distribution diagram (Figure 5) of the samples and their sizes were prepared using ImageJ software. Intriguingly, the results revealed a distinct trend, with GO-3% exhibiting the smallest mean particles size within the range of 30~40 nm. This result suggests that 3% as the optimum weight percentage of rCB that result in the smallest mean particle size of GO. However, the mean particle size of GO-5% in the range of 100~120 nm, suggesting that the higher weight percentage of rCB lead to increase in the particle size of the synthesized GO.

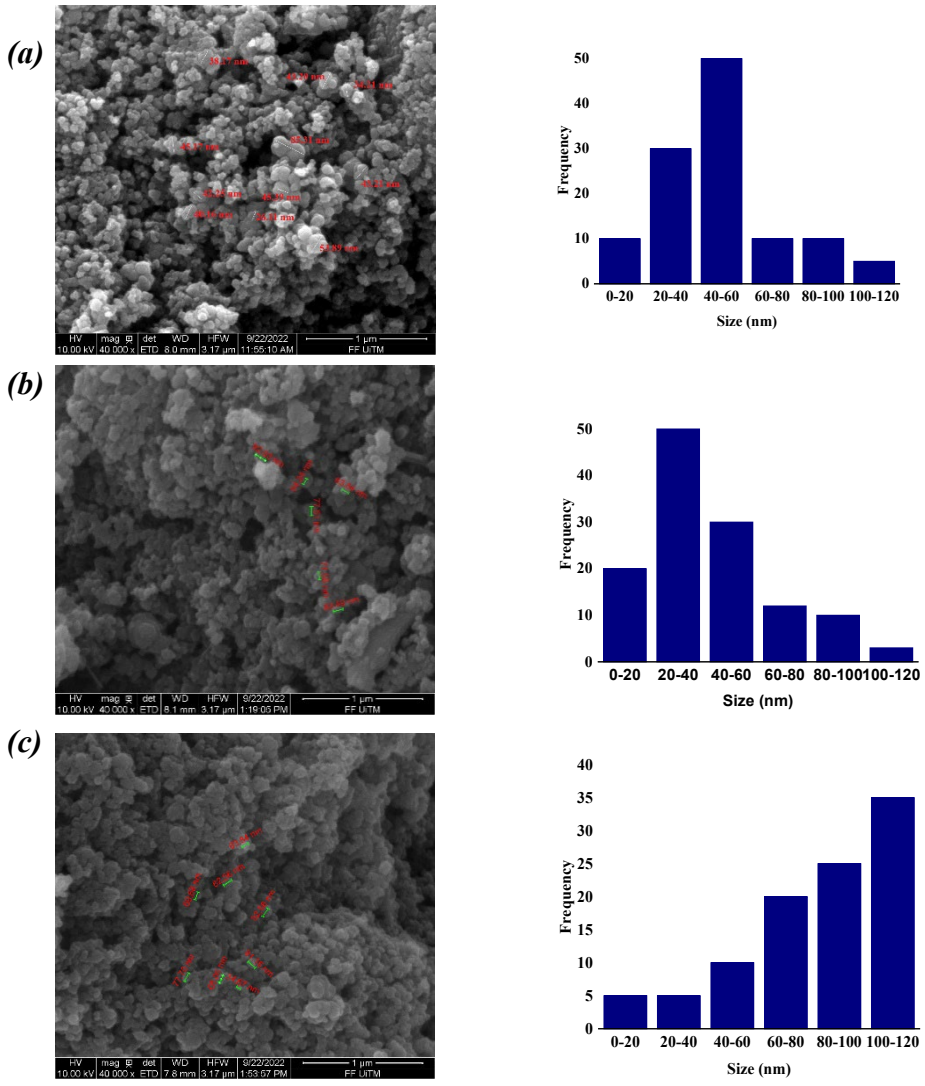

Figure 5: Particle size distribution of GO, obtained by each randomly analyzing ~100 particles size. (a) GO-1%, (b) GO-3%, and (c) GO-5%

4. CONCLUSIONS

The GO with comparable structural and morphological properties was successfully synthesized from different weight percentage of rCB. By adjusting the weight percentage of the source for GO, rCB, using a modified Hummers method, this study effectively suggested

a straightforward and cost-effective synthesis method with improved structural and morphological properties. Through a systematic analysis, it was observed that varying percentages of rCB had a discernible impact on the structural and morphological properties of GO. The FT-IR spectra revealed distinctive peaks corresponding to hydroxyl, carboxyl, and epoxy functional groups, indicative of successful oxidation and functionalization in GO-1%, GO-3%, and GO-5%. The presence of D-band peak at 1359, 1357 and 1355 cm^{-1} and G-band peak at 1618, 1585 and 1583 cm^{-1} for GO-1%, GO-3%, and GO-5% further confirm the formation of GO. Additionally, the intensity ratio (I_d/I_g) of GO-3% demonstrated the highest value of 0.82 indicate the highest degree of oxidation with more defects occur on the structure of GO-3%. Next, XRD analyses shows that the GO-1%, GO-3%, and GO-5% are in amorphous phase with the highest interlayer spacing between graphene layers was recorded for GO-3% with 2.93 Å indicate the highest penetration of the oxygen functional group and structural defects during the chemical oxidation process of rCB. Next, FESEM analysis demonstrate the structure of grain for GO-1% and GO-3% clumps together with several defects occur after the oxidation process. Our results show that the 3 wt% of rCB as the optimum weight percentage source to synthesis GO with high oxidation level with higher oxygenated functional group. This study also demonstrated that the structural and morphological properties of GO can be tunable by incorporating different weight percentages of rCB, thus highlighting the potential for optimizing the use of waste derived from waste tires as a sustainable precursor in graphene-based material synthesis.

Acknowledgements

The authors would like to thank the Ministry of Higher Education Malaysia for their financial assistance and support of this project through the Fundamental Research Grant Scheme (FRGS/1/2021/STG05/UITM/02/16). The authors thank the Faculty of Applied Sciences at Universiti Teknologi MARA (UiTM) Shah Alam for giving us access to their research equipment and facilities.

Author Contributions

All authors contributed toward data analysis, drafting, and critically revising the paper and agree to be accountable for all aspects of the work.

Disclosure of Conflict of Interest

The authors have no disclosures to declare

Compliance with Ethical Standards

Not Applicable

References

[1] Tiwari, S. K., Sahoo, S., Wang, N. & Huczko, A. (2020). Graphene Research and Their Outputs: Status and Prospect. *Journal of Science: Advanced Materials and Devices*, 5(1), 10–29.

[2] Guerrero-Contreras, J. & Caballero-Briones, F. (2015). Graphene Oxide Powders with Different Oxidation Degree, Prepared by Synthesis Variations of the Hummers Method. *Materials Chemistry and Physics*, 153, 209–220.

[3] Ferronato, N. & Torretta, V. (2019). Waste Mismanagement in Developing Countries: A Review of Global Issues. *International Journal of Environmental Research and Public Health*, 16(6), 1060.

[4] Hou, Y., Lv, S., Liu, L. & Liu, X. (2020). High-quality Preparation of Graphene Oxide via the Hummers' Method: Understanding the Roles of the Intercalator, Oxidant, and Graphite Particle Size. *Ceramics International*, 46(2), 2392–2402.

[5] Aixart, J., Díaz, F., Llorca, J. & Rosell-Llompart, J. (2021). Increasing Reaction Time in Hummers' Method Towards Well Exfoliated Graphene Oxide of Low Oxidation Degree. *Ceramics International*, 47(15), 22130–22137.

[6] Anuar, A. U., Bonnia, N. N., Jamil, N. M. & Affandi, N. D. N. (2023). Graphene Oxide Based Regenerated Carbon Waste Tyre (RCB): Synthesis by modified Hummers Method and characterization. *Materials Today: Proceedings*.

[7] Kumar, V., Kumar, A., Lee, D.-J., & Park, S.-S. (2021). Estimation of number of graphene layers using different methods: A focused review. *Materials*, *14*(16), 4590.

[8] King, A. A., Davies, B. R., Noorbehesht, N., Newman, P., Church, T. L., Harris, A. T., Razal, J. M. & Minett, A. I. (2016). A New Raman Metric for the Characterisation of Graphene Oxide and Its Derivatives. *Scientific Reports*, 6(1), 19491.

[9] King, A. A., Davies, B. R., Noorbehesht, N., Newman, P., Church, T. L., Harris, A. T., Razal, J. M., & Minett, A. I. (2016). A new Raman metric for the characterisation of graphene oxide and its derivatives. *Scientific Reports*, *6*(1).

[10] Papanai, G. S., Sharma, I., & Gupta, B. K. (2020). Probing number of layers and quality assessment of mechanically exfoliated graphene via Raman fingerprint. *Materials Today Communications*, *22*, 100795.

[11] Sujiono, E. H., Zurnansyah, Zabrian, D., Dahlan, M. Y., Amin, B. D., Samnur & Agus, J. (2020). Graphene Oxide-Based Coconut Shell Waste: Synthesis by modified Hummers Method and characterization. *Heliyon*, 6(8), e04568.

[12] Le, H. N., Thai, D., Nguyen, T. T., Dao, T. B., Nguyen, T. D., Tieu, D. T. & Ha Thuc, C. N. (2023). Improving Safety and Efficiency in Graphene Oxide Production Technology. *Journal of Materials Research and Technology*, 24, 4440–4453.

[13] Liou, T.-H. & Wang, P. -Y. (2020). Utilization of Rice Husk Wastes in Synthesis of Graphene Oxide-Based Carbonaceous Nanocomposites. *Waste Management*, 108, 51–61.

[14] Jurkiewicz, K., Pawlyta, M. & Burian, A. (2018). Structure of Carbon Materials Explored by Local Transmission Electron Microscopy and Global Powder Diffraction Probes. *C- Journal of Carbon Research*, 4(4), 68.

[15] Saba, N., Jawaid, M., Alothman, O. Y. & Almutairi, Z. (2019). Evaluation of Dynamic Properties of Nano Oil Palm Empty Fruit Bunch Filler/Epoxy Composites. *Journal of Materials Research and Technology*, 8(1), 1470–1475.

[16] Tsugawa, T., Hatakeyama, K., Matsuda, J., Koinuma, M. & Ida, S. (2021). Synthesis of Oxygen Functional Group-controlled Monolayer Graphene Oxide. *Bulletin of the Chemical Society of Japan*, 94(9), 2195–2201.

[17] Festinger, N., Kisielewska, A., Burnat, B., Ranoszek-Soliwoda, K., Grobelny, J., Koszelska, K., Guziejewski, D., & Smarzewska, S. (2022). The influence of graphene oxide composition on properties of surface-modified metal electrodes. *Materials*, *15*(21), 7684.

[18] Al-otaibi, W., Alandis, N. M., Al-Mohammad, Y. M., & Alam, M. (2023). Advanced anticorrosive graphene oxide-doped organic-inorganic hybrid nanocomposite coating derived from Leucaena leucocephala oil. *Polymers*, *15*(22), 4390.

[19] Faniyi, I. O., Fasakin, O., Olofinjana, B., Adekunle, A. S., Oluwasusi, T. V., Eleruja, M. A., & Ajayi, E. O. (2019). The comparative analyses of reduced graphene oxide (RGO) prepared via green, mild and chemical approaches. *SN Applied Sciences*, *1*(10).